

Towards the high-accuracy determination of the ^{238}U fission cross section at the threshold region at CERN – n_TOF

M.Diakaki^{1,a}, L.Audouin², E.Berthoumieux¹, M.Calviani³, N.Colonna⁴, E.Dupont¹, I.Duran⁵, F.Gunsing^{1,3}, E.Leal-Cidoncha⁵, C.Le Naour², L.S.Leong^{2,6}, M.Mastromarco⁴, C.Paradela^{5,7}, D.Tarrio^{5,8}, L.Tassan-Gof², G.Aerts¹, S.Altstadt⁹, H.Alvarez⁵, F.Alvarez-Velarde¹⁰, S.Andriamonje¹, J.Andrzejewski¹¹, G.Badurek¹², M.Barbagallo⁴, P.Baumann¹³, V.Becares¹⁰, F.Becvar¹⁴, F.Belloni⁷, B.Berthier², J.Billowes¹⁵, V.Boccone³, D.Bosnar¹⁶, M.Brugger³, F.Calvino¹⁷, D.Cano-Ott¹⁰, R.Capote¹⁸, C.Carrapico¹⁹, P.Cennini²³, F.Cerutti³, E.Chiaveri³, M.Chin³, G.Cortes²⁰, M.A.Cortes-Giraldo²¹, L.Cosentino²², A.Couture²³, J.Cox²³, S.David², I.Dillmann²⁴, C.Domingo-Pardo²⁵, R.Dressler²⁶, W.Dridi¹, C.Eleftheriadis²⁷, M.Embid-Segura¹⁰, L.Ferrant², A.Ferrari²⁵, P.Finocchiaro²², K.Fraval¹, K.Fujii²⁸, W.Furman²⁹, S.Ganesan³⁰, A.R.Garcia¹⁰, G.Giubrone²⁵, M.B.Gomez-Hornillos²⁰, I.F.Goncalves¹⁹, E.Gonzalez-Romero¹⁰, A.Goverdovski³¹, F.Gramegna³², E.Griesmayer¹², C.Guerrero³, P.Gurusamy³⁰, R.Haight³³, M.Heil²⁴, S.Heinitz²⁶, M.Igashira³⁴, S.Isaev², D.G.Jenkins³⁵, E.Jericha¹², Y.Kadi³, F.Kaepfeler²⁴, D.Karadimos³⁶, D.Karamanis³⁶, M.Kerveno¹³, V.Ketlerov³¹, N.Kivel²⁶, M.Kokkoris³⁷, V.Konovalov³¹, M.Krticka¹⁴, J.Kroll¹⁴, C.Lampoudis²⁷, C.Langer⁹, C.Lederer⁹, H.Leeb¹², S.Lo Meo³⁸, R.Losito³, M.Lozano²¹, A.Manousos²⁷, J.Marganec¹¹, T.Martinez¹⁰, S.Marrone⁴, C.Massimi³⁹, P.Mastinu³², E.Mendoza¹⁰, A.Mengoni³⁸, P.M.Milazzo²⁸, F.Mingrone³⁹, M.Mirea⁴⁰, W.Mondelaers⁷, C.Moreau²⁸, M.Mosconi²⁴, A.Musumarra⁴¹, S.O'Brien²³, J.Pancin¹, N.Patronis³⁶, A.Pavlik⁴², P.Pavlopoulos³, J.Perkowski¹¹, L.Perrot¹, M.T.Pigni¹², R.Plag²⁴, A.Plompen⁷, L.Plukis¹, A.Poch¹⁷, C.Pretel¹⁷, J.Praena²¹, J.Quesada²¹, T.Rauscher^{43,44}, R.Reifarh⁹, A.Riego²², F.Roman³, G.Rudolf¹³, C.Rubbia³, P.Rullhusen⁷, J.Salgado¹⁹, C.Santos¹⁹, L.Sarchiapone³, R.Sarmiento¹⁹, A.Saxena³⁰, P.Schillebeeckx⁷, S.Schmidt⁹, D.Schumann²⁶, C.Stephan², G.Tagliente⁴, J.L.Tain²⁵, L.Tavora¹⁹, R.Terlizzi⁴, A.Tsinganis³, S.Valenta¹⁴, G.Vannin³⁹, V.Variale⁴, P.Vaz¹⁹, A.Ventura³⁹, R.Versaci³, M.J.Vermeulen³⁵, D.Villamarin¹⁰, M.C.Vincente¹⁰, V.Vlachoudis³, R.Vlastou³⁷, F.Voss²⁴, A.Wallner⁴⁵, S.Walter²⁴, T.Ware¹⁵, M.Weigand⁹, C.Weiß³, M.Wiesher²³, K.Wisshak²⁴, T.Wright¹⁵, P.Zugec¹⁶

¹CEA, Saclay, Irfu/SPHn, Gif-sur-Yvette, France ; ²CNRS/IN2P3 – IPN, Orsay, France ; ³CERN, Geneva, Switzerland ; ⁴INFN, Bari, Italy ; ⁵Universidad de Santiago de Compostela, Spain ; ⁶JAEA, Japan ; ⁷EC JRC, IRMM, Geel, Belgium ; ⁸Department of Physics and Astronomy, Uppsala University, Sweden ; ⁹Johann-Wolfgang-Goethe Universität, Frankfurt, Germany ; ¹⁰CIEMAT, Madrid, Spain ; ¹¹University of Lodz, Poland ; ¹²Atominstytut der Österreichischen Universitäten, Technische Universität Wien, Austria ; ¹³CNRS/IN2P3 – IPHC, Strasbourg, France ; ¹⁴Charles University, Prague, Czech Republic ; ¹⁵University of Manchester, UK ; ¹⁶Department of Physics, Faculty of Science, University of Zagreb, Croatia ; ¹⁷Universidad Politécnica de Madrid, Spain ; ¹⁸IAEA Nuclear Data Section, Vienna, Austria ; ¹⁹Instituto Superior Técnico/CTN, Universidade de Lisboa, Portugal ; ²⁰Universitat Politècnica de Catalunya, Barcelona, Spain ; ²¹Universidad de Sevilla, Spain ; ²²INFN – Laboratori Nazionali del Sud, Catania, Italy ; ²³University of Notre Dame, Indiana, USA ; ²⁴KIT, Karlsruhe, Germany ; ²⁵Instituto de Física Corpuscular, CSIC-Universidad de Valencia, Spain ; ²⁶PSI, Villigen, Switzerland ; ²⁷Aristotle University of Thessaloniki, Greece ; ²⁸INFN, Trieste, Italy ; ²⁹JINR, Dubna, Russia ; ³⁰BARC, Mumbai, India ; ³¹IPPE, Obninsk, Russia ; ³²INFN – Laboratori Nazionali di Legnaro, Italy ; ³³LANL, New Mexico, USA ; ³⁴Tokyo Institute of Technology, Japan ; ³⁵University of York, United Kingdom ; ³⁶University of Ioannina, Greece ; ³⁷National Technical University of Athens, Greece ; ³⁸ENEA, Bologna, Italy ; ³⁹Dipartimento di Fisica, Università di Bologna, and Sezione INFN di Bologna, Italy ; ⁴⁰Horia Hulubei National Institute of Physics and Nuclear Engineering, Bucharest - Magurele, Romania ; ⁴¹Dipartimento di Fisica e Astronomia, Università di Catania and INFN-Laboratori Nazionali del Sud, Catania, Italy ; ⁴²University of Vienna, Faculty of Physics, Austria ; ⁴³Centre for Astrophysics Research, School of Physics, Astronomy, Mathematics, University of Hertfordshire, UK ; ⁴⁴Department of Physics, University of Basel, Switzerland ; ⁴⁵Research School of Physics and Engineering, Australian National University, Australia

^a Corresponding author: maria.diakaki@cea.fr

Abstract. The ^{238}U fission cross section is an international standard beyond 2 MeV where the fission plateau starts. However, due to its importance in fission reactors, this cross-section should be very accurately known also in the threshold region below 2 MeV. The ^{238}U fission cross section has been measured relative to the ^{235}U fission cross section at CERN – n_TOF with different detection systems. These datasets have been collected and suitably combined to increase the counting statistics in the threshold region from about 300 keV up to 3 MeV. The results are compared with other experimental data, evaluated libraries, and the IAEA standards.

1 Introduction

The fission cross sections of ^{235}U and ^{238}U are of fundamental importance in the field of nuclear technology, as well as for other fields of basic and applied nuclear physics. In particular, fission cross section in the hundreds-of-keV region are of paramount importance for the development of innovative fast reactors. The $^{235}\text{U}(n,f)$ cross section is an international standard at 0.0253 eV and above 0.15 MeV, and $^{238}\text{U}(n,f)$ is a standard beyond 2 MeV [1]. While the $^{235}\text{U}(n,f)$ standard is commonly used for neutron flux measurements from thermal to high energy, the $^{238}\text{U}(n,f)$ threshold cross section can be more conveniently used in the presence of a low energy neutron background.

To address the need of new and accurate data for future improvements of these standards a series of measurements of the $^{238}\text{U}(n,f)/^{235}\text{U}(n,f)$ cross section ratio were performed at the CERN n_TOF facility up to 1 GeV. Some of these measurements are described in detail in Ref. [2]. In the present contribution, the results of one more dataset are included, and the possibility to obtain high accuracy $^{238}\text{U}(n,f)$ cross section results at the threshold (0.3 MeV - 3 MeV) is examined.

2 Experimental setups

The measurements were performed at the CERN n_TOF facility [3–7], which is based on the spallation of 20 GeV/c protons on a lead target. Data were collected in different campaigns from the experimental area 1 (EAR1) approximately 190 m downstream of the neutron source. Two detection setups were used: a fast fission ionization chamber (FIC), in which a single fission fragment (FF) is detected, and an array of parallel plate avalanche counters (PPAC), in which the two FFs are detected in coincidence.

2.1 The Parallel Plate Avalanche Counters

The PPAC are gaseous detectors with very thin windows, small gaps between electrodes and low gas pressure [8-11]. These features make the detector practically insensitive to the prompt γ -flash. The actinide samples were deposited on very thin backings and positioned between two PPACs for measuring FFs in coincidence. The main advantage of the coincidence technique is the very high efficiency for rejecting the α -particle background from the sample, as well as for discriminating fission against competing reactions. Another advantage of PPACs is that they can also measure the angular distribution of FFs. The main drawback of the system is the limited angular acceptance and the angular dependence of the efficiency.

In the first experimental campaign the PPAC detectors were mounted perpendicular to the neutron beam direction, hereafter referred to as “PPAC perpendicular”. In this configuration the setup is affected by a loss of efficiency for FFs emitted at angles larger than $\sim 60^\circ$. To overcome this problem, a new geometrical configuration was adopted in a second campaign, with the detectors and the samples tilted by 45° . Two measurements were performed with the tilted setup, hereafter referred to as “PPAC tilted 1” and “PPAC tilted 2”. Details on the analysis of the data in each configuration can be found in [2,8-14]. The PPAC samples were prepared at IPN (Orsay, France), and most of the targets used were characterised by means of alpha spectroscopy and Rutherford Backscattering Spectrometry (RBS).

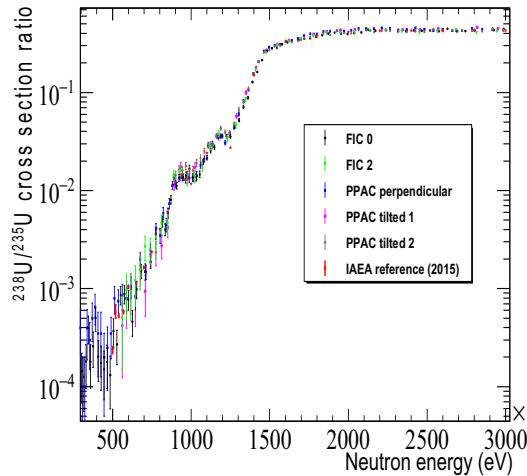


Figure 1. The $^{238}\text{U}/^{235}\text{U}$ fission cross-section ratio measured at n_TOF with the different detection systems, in the neutron energy range 0.3-3MeV. The statistical uncertainties are plotted. The ratio calculated based on the IAEA references (2015) is shown for comparison.

2.2 The Fast Ionization Chamber

The fast ionization chamber [15-16] is made of a stack of ionization cells consisting of two external electrodes and a central electrode plated on both sides with the fissile deposit. The FIC0 and FIC1 versions of the detector were specifically built as “sealed sources” for measurements of highly radioactive samples. The FIC2 was used as a neutron flux monitor, thus it was much lighter and directly coupled to the vacuum tube. The samples were prepared using the painting technique at the IPPE (Obninsk, Russia) and the JINR (Dubna, Russia), and most of the targets used were characterised by means of alpha spectroscopy and the RBS technique.

For the extraction of the $^{238}\text{U}(n,f)/^{235}\text{U}(n,f)$ cross section ratio, one ^{238}U and two ^{235}U samples were used from the FIC0 measurements, two ^{235}U and four ^{238}U samples from FIC1, and one ^{238}U and two ^{235}U samples from FIC2. Different analysis procedures and corrections were applied for the data from the different detectors as described in [2,15-18]. The data collected with FIC2 were normalised to the results obtained with the FIC1 chamber in the 1–10 MeV energy region, due to the large uncertainty of the ^{238}U sample mass.

3 Results for the $^{238}\text{U}(n,f)/^{235}\text{U}(n,f)$ cross section ratio measurement

The systematic uncertainties from the different datasets are summarised in Table 1 (assuming a uniform distribution). Fig. 1 shows the results of the different measurements at n_TOF of the $^{238}\text{U}/^{235}\text{U}$ fission cross-section ratio for neutron energies in the range 0.3–3 MeV. A good agreement among the various datasets was observed, within their uncertainties, especially at the first chance fission plateau. Very few differences bigger than 1σ are noticed at the threshold at ~ 1.2 MeV where the systematic uncertainty due to the FF emission anisotropy becomes larger.

Each of the five datasets collected at n_TOF represents a new result by itself, and should be considered independently from each other, for re-evaluating the fission cross section ratio. Nevertheless, in order to compare the n_TOF data with previous measurements and current evaluations, the n_TOF $^{238}\text{U}/^{235}\text{U}$ fission cross section ratio has been calculated as the weighted average value of all the datasets, taking into account the uncorrelated statistical uncertainties. Firstly, all the datasets were normalised to the ratio calculated with the IAEA standards (2006) in the energy range 2.2-2.6 MeV, and the normalisation factor did not exceed 3%. An energy shift was applied to all

the datasets in order for them to match in the energy region of 1.34-1.48 MeV where the slope of the $^{238}\text{U}(n,f)$ cross section is largest. This energy-matching shift was less than 0.7%. A binning of 50 bins/decade was chosen for $E > 800$ keV and 25 bins/decade for $E < 800$ keV, and a linear interpolation was applied between consecutive points in order to match this binning.

Table 1. Systematic uncertainties (in %) on the data collected in the measurements of the $^{238}\text{U}/^{235}\text{U}$ fission cross-section ratio. Since the same samples were used in the “perpendicular” and “tilted 1” PPAC measurements, the corresponding uncertainties on the sample mass are fully correlated. For the last dataset, normalized to ENDF/B-VII.1 (see [2]), the uncertainty in the mass is replaced by the one in the evaluated cross sections.

Setup	Samples	Efficiency	Dead-time
FIC 0	2	1-2	<0.5
FIC 1, 2	1.5	1	<3
PPAC perpendicular	1.1	3	< 1
PPAC tilted 1	1.1	2	< 1
PPAC tilted 2	(~1)	1	< 1

The extracted n_{TOF} $^{238}\text{U}/^{235}\text{U}$ fission cross section ratio is shown in Fig. 2, along with experimental data from the EXFOR database [19] and major evaluations, as well as the associated residuals divided by 1σ (statistical uncertainty). The systematic uncertainty of the weighted average ratio, taking into account the normalisation to the IAEA standards, can be calculated from the energy-dependent uncertainties given in Table 1 and is roughly estimated to be less than 1.5% (1σ).

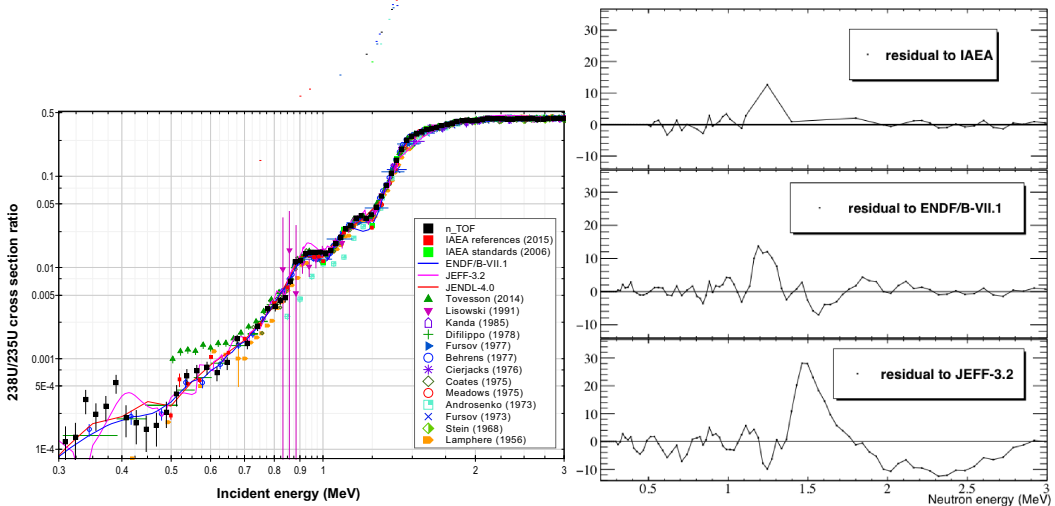


Figure 2. a) The $^{238}\text{U}/^{235}\text{U}(n,f)$ cross section ratio obtained from the weighted average of the n_{TOF} datasets compared with the IAEA standard (2006) and reference (2015) and major evaluations, as well as data available in EXFOR. b) The residual of the n_{TOF} dataset with selected references and evaluations, divided by 1σ (statistical) of the n_{TOF} dataset.

It can be noted that at the threshold region the evaluations present differences $>5\sigma$ from the n_{TOF} data, and that below ~ 750 keV the latest data of Tovesson (2014) are systematically above the n_{TOF} data.

4 Determination of the $^{238}\text{U}(n,f)$ cross section

Based on the merged n_TOF dataset and the IAEA (2006) standard $^{235}\text{U}(n,f)$ cross section, the $^{238}\text{U}(n,f)$ cross section was extracted at the threshold region. It is shown in Fig.3, along with selected previous data available in the EXFOR database.

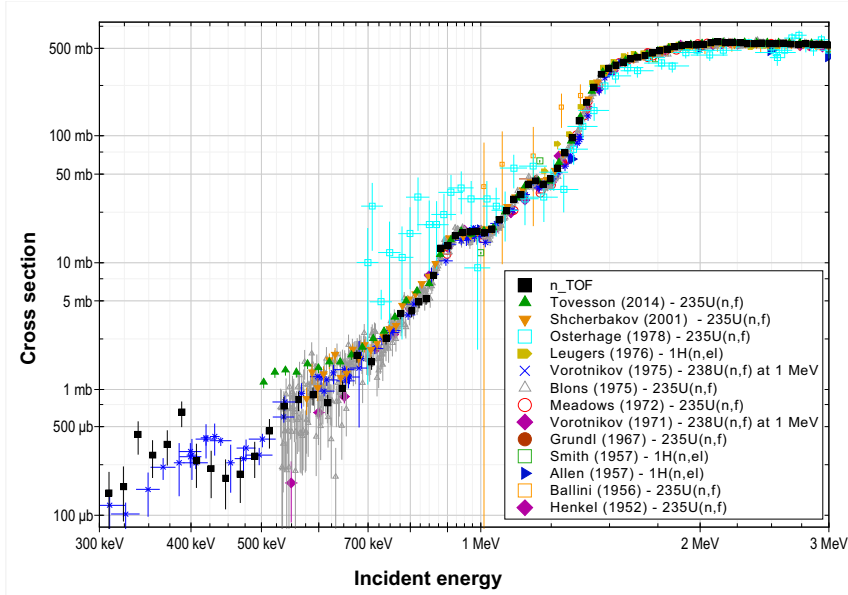


Figure 3. The $^{238}\text{U}(n,f)$ reaction cross section in the energy range 0.3-3MeV measured with reference to the $^{235}\text{U}(n,f)$ cross section at n_TOF (black squares), along with experimental data available in the EXFOR database. Next to the label the reference reaction used is noted.

The n_TOF data extracted with $^{235}\text{U}(n,f)$ as a reference agree within 1σ with most other datasets extracted with the same reference, as well as with the data from Allen (1957) using $^1\text{H}(n,el)$ as reference. Only a few other datasets exist at the threshold region with reference to the $^1\text{H}(n,el)$, (such as Smith (1957) and Leugers (1976)) but for $E < 1.5$ MeV they present differences bigger than 1σ with respect to all available data using the $^{235}\text{U}(n,f)$ as reference.

Despite the statistical uncertainties, interesting shoulders can be noticed in the threshold region at ~ 0.4 , ~ 0.6 , ~ 0.8 , ~ 1 , and ~ 1.2 MeV, most of them not properly described in the latest evaluations and worth being studied in the context of the fission barrier parameters related to different fission modes, resonant sub-threshold structure, etc. [20] as well as to the competition with the inelastic neutron channel.

5 Outlook

The $^{238}\text{U}/^{235}\text{U}$ fission cross section ratio has been measured at n_TOF with two different detection systems, one of which was used in two different geometrical configurations. The results of the measurements are consistent within their combined uncertainties. The datasets have been combined in order to obtain a unique dataset and the $^{238}\text{U}(n,f)$ cross section was derived. The extracted ratio could be used to improve the accuracy of current libraries, and in particular of the IAEA standard and of reference datasets used in a variety of applications. New measurements of the $^{238}\text{U}/^{235}\text{U}$ fission cross section ratio are foreseen using the new vertical neutron beam line of the n_TOF facility [21] with much higher statistics in the region of the threshold, especially for neutron energies below 0.5 MeV.

References

1. A. Carlson et al., Nuclear Data Sheets **110**, 3215 (2009).
2. C. Paradela et al., Phys. Rev. C **91**, 024602 (2015).
3. <http://www.cern.ch/ntof>.
4. U. Abbondanno et al., CERN/INTC-O-011 INTC-2002-037, CERN-SL-2002-053 ECT (2003).
5. C. Guerrero et al., Eur. Phys. J. A **49**, 27 (2013).
6. M. Barbagallo et al., Eur. Phys. J. A **49**, 156 (2013).
7. N. Colonna et al., Energy Environ. Sci. **3**, 1910 (2010).
8. C. Paradela et al., Phys. Rev. C **82**, 034601 (2010).
9. D. Tarrío et al., Nucl. Instr. Meth. A **743**, 79 (2014).
10. C. Paradela, I. Duran, D. Tarrío, L. Audouin, L. Tassan-Got, and C. Stephan, *Proceedings of the 2nd International Conference on Advancements in Nuclear Instrumentation Measurement Methods and their Applications (ANIMMA)*, June, 2011, Ghent, Belgium, pp. 6–9 (IEEE, 2011).
11. D. Tarrío et al., Nucl. Data Sheets **119**, 35 (2014).
12. D. Tarrío et al., Phys. Rev. C **83**, 044620 (2011).
13. D. Tarrío, PhD thesis, Universidade de Santiago de Compostela, Spain (2012).
14. L.S. Leong, PhD thesis, University of Paris-Sud, France (2013).
15. M. Calviani et al., Nucl. Instr. Meth. A **594**, 220 (2008).
16. M. Calviani et al., Phys. Rev. C **80**, 044604 (2009).
17. D. Karadimos et al., Nucl. Instr. Meth. B **268**, 2556 (2010).
18. D. Karadimos et al., Phys. Rev. C **89**, 044606 (2014).
19. N. Otuka et al., Nuclear Data Sheets **120**, 272 (2014).
20. E. Birgesson et al., Nucl. Phys. A **817**, 1 (2009).
21. C. Weiss et al., Nucl. Instr. Meth. A **799**, 90 (2015).